

Water retention behaviour of tailings in unsaturated conditions

Gianluca Bella^{*1,2}

¹Politecnico di Torino, C.so Duca degli Abruzzi 24, Torino, Italy

²Pini Swiss Engineers, Via Besso 7, Lugano, Switzerland

(Received April 20, 2020, Revised June 18, 2021, Accepted June 26, 2021)

Abstract. Tailing dams are complex geotechnical systems comprising of an embankment and a basin containing the waste products from the mining processes. These structures are characterized by a wide surface exposed to the atmosphere whose interaction governs the position of the phreatic surface within the basin. A detailed knowledge of the hydro-mechanical properties of the tailings is fundamental to reliably assess the stability of the tailing dams. While most of the previous studies have dealt with the response of tailings in saturated conditions, this research provides an extension of the hydraulic behaviour in unsaturated and nearly saturated state of tailings collected after the failure of the Stava basins. The hydraulic behaviour in unsaturated conditions was investigated by means of tests where the suction was imposed and the water content was monitored (axis translation technique and vapour equilibrium technique), and tests where the water content was imposed and the suction was measured with psychrometer (dew point method). To account for the in-situ heterogeneity of tailings, the dependency of the water retention relationship on the grain size distribution, the preparation technique and on the initial density / void ratio was studied. Denser tailings showed a higher water retention behaviour than that given in looser specimens. Similarly, the increase of the fine content was demonstrated to improve the water retention capability. As for standard soils, also statically compacted Stava tailings reveal lower retention capability than the slurry samples, thus confirming the importance of the preparation method in determining the hydro-mechanical response of such soils.

Keywords: fine content; soil water retention curve; tailing dams; unsaturated soil; void ratio

1. Introduction

Tailings are the waste products resulting from the chemical and the mechanical separation processes of mineral extraction. Comprising of mixtures of crushed rocks and processing fluids, their particle size ranges from sand to clay/silt size. Surface storage facilities for the disposal of wet tailings are known as tailings dams (Fig. 1(a)) and represent some of the largest and complex geotechnical structures in the world. These structures usually comprise of a raised earth embankment constructed in stages over the life of the impoundment, and a basin aimed to store billions of tons of tailing materials. According to the classical hydraulic segregation profile, a higher permeability zone made up of coarse particles would exist near the embankment/discharge point, with a lower permeability zone (pond) made up of fine particles furthest from this point, and between them there is an intermediate permeability zone (beach).

The high rate of historical and recent collapses poses serious environmental threats when the mine closes or is still active, causing human loss of lives (Fig. 1(a)), environmental and economic damages (Fig. 1(b), Fig. 1(c)).

Tailing basins are heterogeneous systems subjected to many external factors affecting their operation (Alonso and Gens 2006, Bhanbhro 2014, Zuoan *et al.* 2019), i.e.,

amount of surface runoff, infiltration rate, consolidation process, or capillarity rise (Fig. 2(a)). These factors, caused by interactions with the atmosphere, govern the position of the phreatic surface within the basin, leading to variations in the height of the unsaturated zone above the water table. The soil below the phreatic level is usually saturated and the pore water pressure is positive, whilst above the phreatic surface there is a capillary fringe consisting of saturated zone with a negative pore water pressure. An unsaturated region with a negative pore water pressure and a degree of saturation less than 100% lies above the saturated capillary fringe (Fig. 2(c)).

The importance of understanding the behaviour of soils in the unsaturated portion of the ground is recognized in engineering practice. However, a gap still exists between engineering practice and research in unsaturated soil mechanics, mainly because it requires sophisticated apparatus and time-consuming experimental methodologies. Despite this, the unsaturated conditions of tailings are fundamental tools to understand the climate effects on tailing dams. These include the consequences of rainfall, snowmelt, or poor management on the stability of an embankment of which these are considered some of the main worldwide causes of failure (Rico *et al.* 2008, Zanardin *et al.* 2009).

Hydraulic and mechanical behaviour in unsaturated conditions is coupled (Alonso 1990, Tarantino and Tomblato 2005, Lu and Likos 2006, Estabragh and Javadi 2014, Arab *et al.* 2015, Nicotera *et al.* 2015, Kim and Jeong 2017, Horn *et al.* 2018, Deng *et al.* 2020). Therefore, the

*Corresponding author, Ph.D.
E-mail: gianluca.bella@polito.it

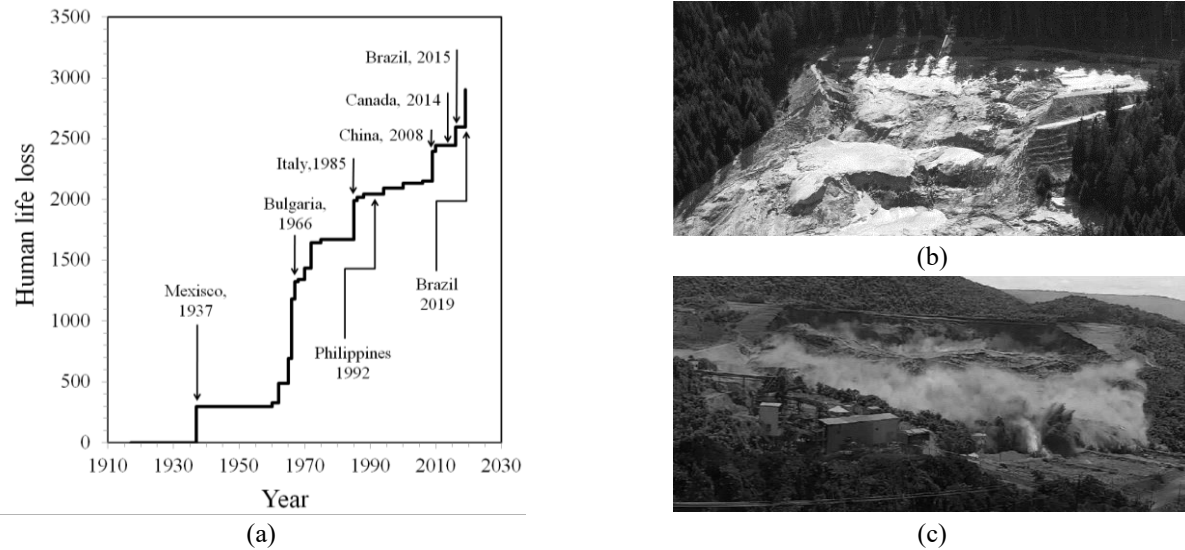


Fig. 1 (a) Numbers of victims associated with the major tailing failures (Santamarina *et al.* 2019); Examples of historical and recent failures: (b) Stava tailing dams - Italy - 1985 (Lucchi, 2020) and (c) Feijão tailing dam - Brazil - 2019 (Robertson *et al.* 2019).

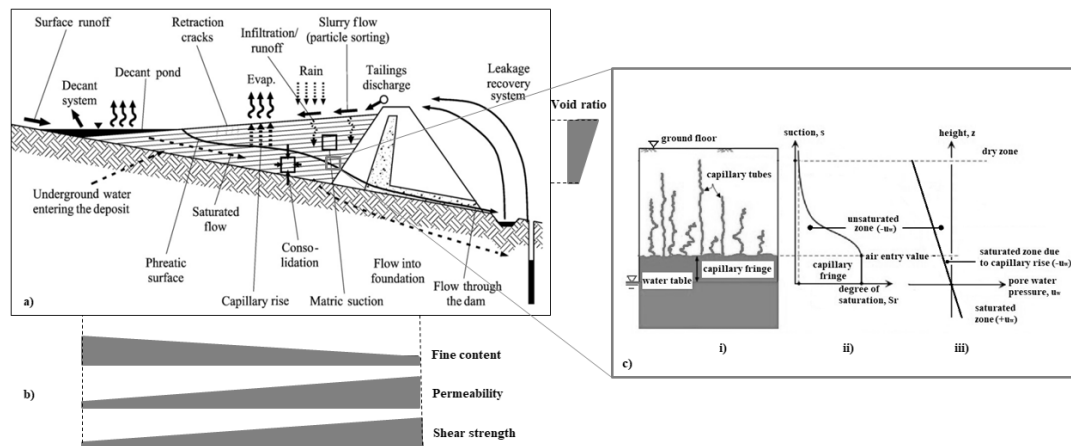


Fig. 2 (a) Representative cross section of a tailing dam, (b) Soil properties with respect to deposition location and (c) Schematic representation (I and II) of the unsaturated conditions and (III) pore water pressure profile in tailing basins, (modified from Zanardin *et al.* 2009)

accuracy in predicting the hydraulic soil response is essential for determining the mechanical soil behaviour in terms of shear strength. Indeed, the pore-fluid affects the shear strength via its suction but also its degree of saturation so, the same suction but with different degrees of saturation will lead to different values of shear strength. A relevant example of stability analysis of tailing dams based on this concept was given by the recent collapse of the Feijão tailing dam (Brazil), where high rainfalls and high infiltrations were proved to decrease the suctions by approx. 50 kPa in the unsaturated zone above the water table, which in turn reduced the shear strength by 10 kPa to 15 kPa, providing one of the cause that supposedly led to the instability of the embankment (Robertson *et al.* 2019).

Over the years several shear strength criteria for unsaturated soils have been proposed in the literature. Some of them were based on regression analyses of experimental data from either triaxial or direct tests (Fredlund *et al.* 1978,

Gan *et al.* 1988, Fredlund *et al.* 1996, Oberg and Sallfors 1997, Khalili and Khabbaz 1998, Rassam and Williams 1999, Rassam and Cook, 2002, Toll and Ong 2003, Tekinsoy *et al.* 2004, Xu 2004). Other strength criteria were proposed within different constitutive models for unsaturated soils (Alonso *et al.* 1990, Sun *et al.* 2000, Sheng *et al.* 2008, Alonso *et al.* 2010). Therefore, the degree of saturation that can be obtained from the water retention curve (WRC) for a certain suction has been embedded into strength criteria for unsaturated soils (Fredlund *et al.* 1996, Vanapalli *et al.* 1996, Oberg and Sallfors 1997, Toll 1990, Toll and Ong 2003). Although some other shear strength criteria for unsaturated soils do not include the degree of saturation explicitly (Khalili and Khabbaz, 1998; Sheng *et al.* 2008), the key parameters involved in these criteria, such as the air-entry value, are embedded in the WRC. Knowledge of the WRC can provide other applications with the estimation of the

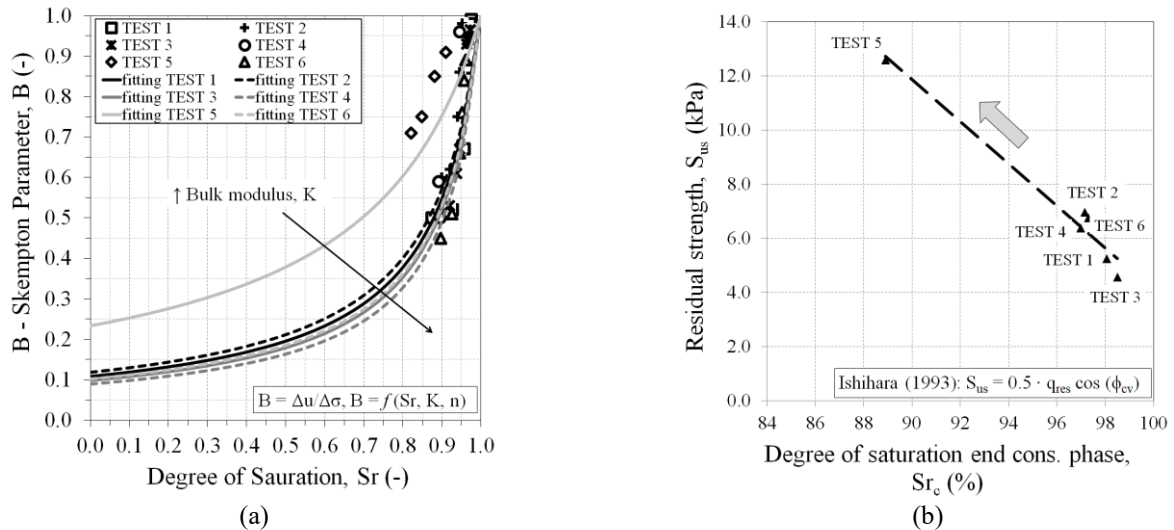


Fig. 3 Application of unsaturated soil mechanics in the stability analysis of Stava tailing dams: (a) relationship between B-Skempton parameter and S_r and (b) variation of the residual strength with the degree of saturation (Bella 2017)



Fig. 4 Stava basins. (a) Geographical localization and (b) sketch: A upper basin, B lower basin, (1) on-dam cyclone for the extraction of the coarser sand components from the tailing wastes, (2) upper beach, (3) upper pond, (4) drainage service, (5) emergency drainage, (6) service road, (7) lower beach, (8) lower pond, (9) drainage from the upper dam, (10) caretaker's house (modified from Luino and De Graff 2012)

hydraulic conductivity of unsaturated tailings, generally expressed by the combination of the saturated hydraulic conductivity and the relative hydraulic conductivity, the latter depends upon the degree of saturation (van Genuchten, 1980). Finally, recent applications of unsaturated soil mechanics regarding tailing dams stability can be found in Bella (2017) with reference to the occurrence of the static liquefaction which is considered one of the main causes of failure. In undrained conditions, when the degree of saturation slightly decreased below the unit due to changes in suction, the excess pore pressure of the unsaturated Stava silty tailings was proved to be much lower than that in saturated conditions (Fig. 3(a)), leading to an increase in the soil's shear strength and so strongly influencing the occurrence of the static liquefaction (Fig. 3(b)).

In summary, an in-depth geotechnical characterization of the hydro-mechanical behaviour of tailings represents a fundamental tool for reliably assessing the stability of tailing dams and therefore in improving their design. For this reason, this study is aimed at providing a preliminary insight into the range of hydraulic behaviour predicted in tailing materials, by taking into account the variation in the density, the particle sorting which could reasonably be expected in situ, and preparation technique. The soil density and grading considered in this study can be related to plausible locations and depths within a basin through a geostatistic approach (Esposito *et al.* 2010). This study provides the basis for defining the spatial distribution of hydraulic variables from a better understanding of the unsaturated behaviour of tailing dams, which, when modelled numerically (Tarantino and Mountassir 2013,

Tarantino and Di Donna 2019) will result in a more accurate evaluation of the tailing dam safety.

2. Testing material

The hydraulic behaviour of the Stava tailings was investigated by means of laboratory tests carried out at the soil laboratory of Politecnico di Torino (Italy) on unsaturated samples. Soil tests are performed on the tailing samples manually collected in 2005 at ground level from the lower portion of the Stava upper dam, which remained in place after the collapse (Fig. 1(b)). The two storage facilities were raised with the upstream technique, built one above the other on a natural slope near village of Stava, Italy (Fig. 4). In July 1985, the lower dam failed due to overtopping caused by the collapse of the upper one and triggering a flow-slide of more than 200'000 m³. The causes of the failure are complex and have been investigated in detail by others (e.g., Chandler and Tosatti, 1995), but the unconsolidated state of the tailings, a poor drainage and the high phreatic level were supposed to be the main factors that caused the static liquefaction, leading the failure of the Stava tailings dam.

3. Material characterization

Tailings used in the current research are composed of two grain sizes: a sand fraction made up of particles retained by sieve n°200, and a silt fraction passing through a sieve n°200 (Fig. 5). This choice was due to the fact that Stava tailings not passing through 0.074 mm sieve (mesh sieve n°200) was part of the embankment, while finer particles seemed to be deposited inside the basin. The D₁₀ of the sand fraction is equal to 0.08 mm, D₅₀ and D₉₀ are 0.20 mm and 0.35 mm, respectively (Carrera *et al.* 2011). Liquid (w_L) and plastic limits (w_P) show that the silty fraction is characterized by medium-low plasticity with 8% in weight

Table 1 Geotechnical index properties of the silty and the sandy fraction: liquid limit (w_L), plastic limit (w_P), plasticity index (PI), specific gravity (G_s) and average absolute permeability (k). (Carrera *et al.* 2011)

Material	w_L (%)	w_P (%)	PI (%)	G_s (-)	k (m/s)
Sandy fraction	-	-	-	2.721	$9.5 \cdot 10^{-6}$
Silty fraction	27.4	18.0	9.4	2.828	10^{-7}

Table 2 Percentages of minerals obtained from the X-ray diffraction analyses (Bella 2017)

Mineral	Silty fraction (% mass)	Sandy fraction (% mass)
Magnetite	-	11.0
Quartz	36.4	70.0
Feldspars K	traces	traces
Feldspars Na	-	traces
Calcite	11.9	6.0
Fluorite	47.8	2.0

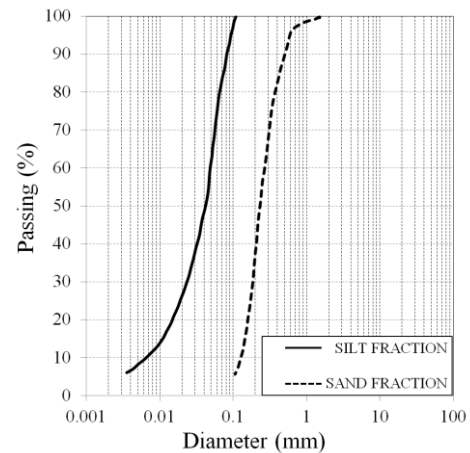


Fig. 5 Grain size distribution of the two fractions of the Stava tailings (modified from Carrera *et al.* 2011)

of clay size material. Results are shown in Table 1, while Table 2 gives the results of the X-ray diffraction analysis. Both fractions were predominantly made up of quartz, with a significant amount of calcite and fluorite, especially within the silty fraction (Bella 2017).

3.1 Sample preparation

The water retention tests were carried out on silt specimens with a different initial void ratio, different preparation techniques and on mixtures of silt and sand.

The axis translation technique was applied in a suction-controlled oedometer on samples having initial size of 50 mm diameter and height of 20 mm. The compacted specimens (Fig. 6(a)) were prepared mixing a required amount of dry soil with a certain amount of demineralized, de-aired water to obtain the target dry density and water content. The mixture was then put in a cylindrical mould, and statically compacted by gradually applying an axial force with a filter paper on the top and bottom of the sample. A control axial displacement Wykeham Farrance loading frame was used to compact the sample until the desired volume was reached under controlled water content. It is worth noting that during the assembling of the mould prior the static compaction phase, two filter papers were placed on the top and bottom face of the sample and grease was applied around the mould wherever the water could drain out preventing water leakage. Furthermore, deceleration of applying the axial load helped to reduce the localized excess pore water pressure generated at sample ends. The statically compacted specimens were finally tested by means of suction-controlled oedometer cell by applying the axis translation technique (Table 3 and Fig. 6(a)):

- pure silt with initial void ratio equal to 0.70 (labelled as SILT-0.70)
- pure silt with initial void ratio equal to 0.60 (labelled as SILT-0.60)
- pure silt with initial void ratio equal to 0.50 (labelled as SILT-0.50)
- mixture 70% sand - 30% silt with initial void ratio equal to 0.70 (labelled as 7030-0.70)

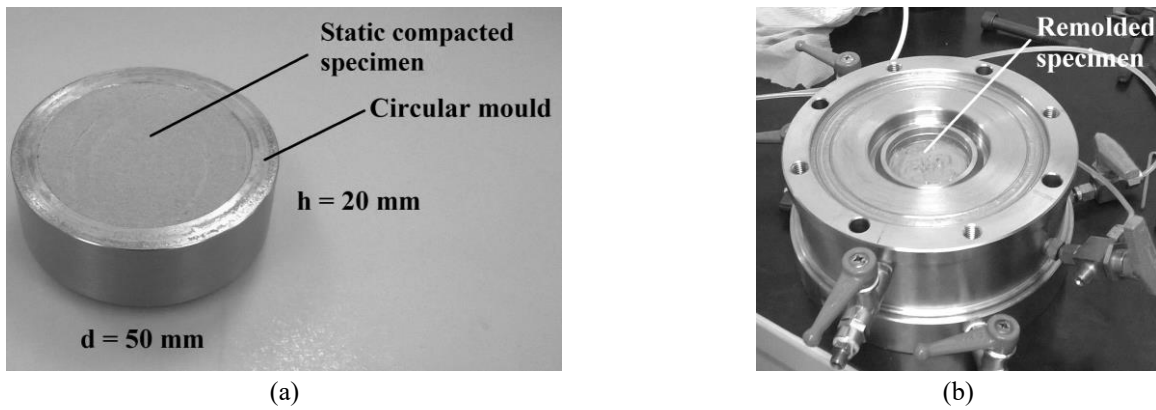


Fig. 6 (a) Statically-compacted sample inside the oedometric ring and (b) Remolded samples inside the suction-controlled oedometer cell

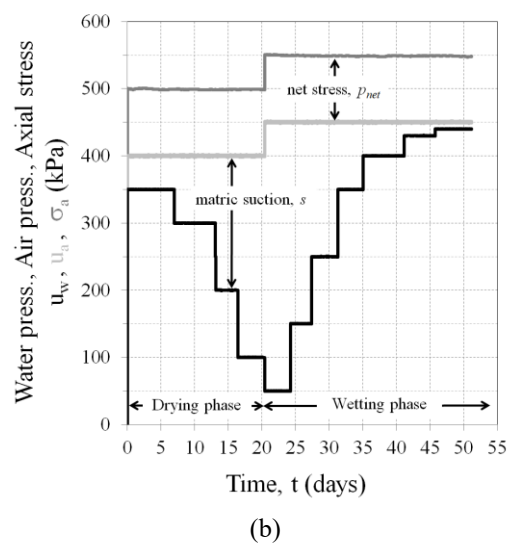
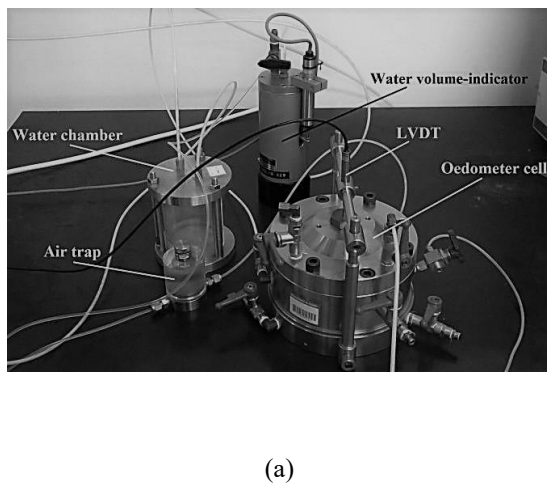


Fig. 7 (a) Suction controlled oedometer and (b) Axial stress, air pressure and water pressure during time for sample SILT-0.70 (modified from Bella 2017)

Table 3 Initial state of specimens: void ratio (e_0), water content (w_0), degree of saturation (Sr_0), dry weight (γ_d), initial net stress (p_{net}), percentage of sand/silt and preparation method (RE = remolded, ST = statically compacted)

Sample	e_0 (-)	w_0 (%)	Sr_0 (%)	γ_d (kN/m ³)	p_{net} (kPa)	Sand (%)	Silt (%)	Preparation method
SLURRY-0.78	0.78	27.4	100.0	15.9	10.0	0	100	RE
SILT-0.70	0.70	17.3	70.0	16.6	100.0	0	100	ST
SILT-0.60	0.60	15.0	70.0	17.6	100.0	0	100	ST
SILT-0.50	0.50	15.9	90.0	18.9	100.0	0	100	ST
7030-0.70	0.70	17.8	70.0	16.2	100.0	70	30	ST
3070-0.60	0.60	17.2	80.0	17.4	100.0	30	70	ST

- mixture 30% sand - 70% silt with initial void ratio equal to 0.60 (labelled as 3070-0.60).

Specimens tested by applying the vapour equilibrium technique and dew point measurements were prepared in the same way and had a diameter of 20 mm and a height of 10 mm.

The remolded specimen (initial size: 50 mm diameter,

20 mm height) was prepared by mixing a required amount of dry soil with a certain amount of demineralized, de-aired water corresponding to the limit liquid, so it assumed the consistence of a slurry. Then, it was placed inside the suction-controlled oedometer cell and tested (axis translation technique) without any static compaction (Fig. 6(b) and Table 3):

- pure slurry silt with initial void ratio equal to 0.78 (labelled as SLURRY-0.78).

3.2 Experimental techniques

The hydraulic characterization of Stava tailing samples was based both on techniques where the suction was imposed and the water content was measured (axis translation and vapour equilibrium technique), and on tests where the water content was imposed and the suction was measured with the dew point method.

The relationship between the water content θ , or degree of saturation Sr and matric suction s was obtained for $s \leq 500$ kPa in a suction controlled oedometer apparatus (Fig. 7(a)), by applying the axis translation technique. The axial

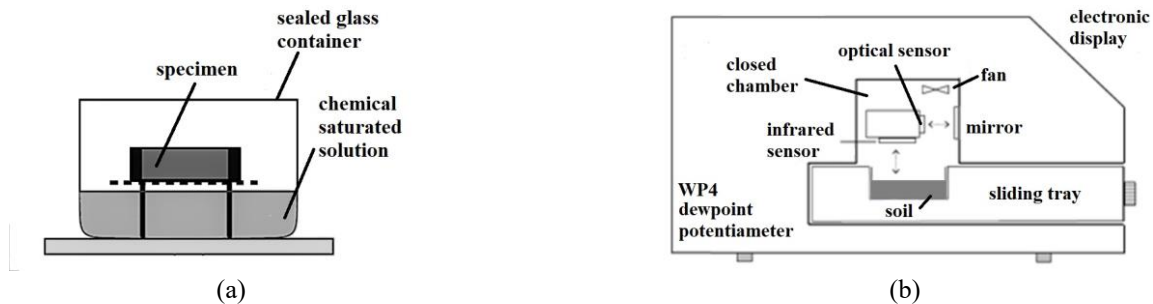


Fig. 8 (a) Schematic view of the equipments used to apply the vapour equilibrium technique and (b) Schematic view of the chilled-mirror psychrometer for dew-point technique (Bulut *et al.* 2002)

displacement of the oedometer samples were measured by using a linear variable differential transducer (LVDT) connected to the top plate. The axial stress (maximum allowed 1.6 MPa) was applied by pressurized air acting on the loading plate. A high Air Entry Value ceramic porous stone ($AEV = 500$ kPa) was located at the bottom of the sample, in order to apply the pore water pressure, while the pore air pressure was applied at the top through a coarse porous stone. An air trap was installed in the water system to avoid the creation of air bubbles close the porous stone at the bottom of the sample. A water chamber was installed in the air system to maintain a high relative humidity of air in order to reduce the evaporation of water vapors. Finally, a water volume-indicator (capacity 50 cc) was connected to the bottom AEV porous stone and allowing to quantify the water volume exchanged by the soil sample during drying and wetting processes.

After the unsaturated static-compacted specimen was placed inside the cell, suction values and net stress were imposed by independent control of the water pressure u_w , air pressure u_a and axial stress σ_a , according to the axis translation technique. The drying phase was realized by maintaining a constant air pressure and decreasing the water pressure step-by-step, until equilibrium, in terms of water volume exchange, was obtained (Fig. 7(b)). On the opposite side, the wetting phase was obtained by increasing the water pressure, until equilibrium conditions were reached. At the end of the drying step, the air pressure had increased by 50 kPa and the water pressure had decreased by 50 kPa to obtain 400 kPa of suction. Consequently, the axial stress σ_a was increased by 50 kPa to maintain a constant net stress during the entire test. It is also worth noting that, to accurately obtain entire WRC for a certain soil sample with the axis translation technique, the entire test can take up to 55 days (Fig. 7(b)).

Suction values up to 70 MPa were imposed at soil specimens 20 mm diameter and 10 mm height through the vapour equilibrium technique (VET). The vapour equilibrium technique was implemented by controlling the relative humidity to impose a desired total suction. In the current study, this method was used at providing additional data for the suction levels out of the axis translation technique range. The desired total suction was imposed by creating a controlled relative humidity condition using the osmotic potential of chemical solutions, as proposed by Romero (1999), and Tang and Cui (2005). These conditions

are usually realized into a sealed glass container with a porous support above the chemical solution, which suspends the soil specimens in the vapour environment (Fig. 8(a)). The total suction within the specimen is obtained due to a net water exchange between the liquid phase within the unsaturated specimen and the vapour phase in the headspace of a box, until equilibrium between the two phases was reached. During the transient phase, the soil sample was weighted at regular intervals until it reached a constant weight, meaning no further variations in water content and suction. In order to minimize any changes in moisture due to room temperature fluctuations, during the experimentation period the temperature and relative humidity RH of the laboratory were accurately monitored and maintained at a constant ($RH = 38.5\%$, $T = 21^\circ\text{C} \pm 0.5^\circ\text{C}$). It is important to note that the vapour equilibrium technique controls the total suction (ψ), that is defined as the sum of two components, matric suction (s) and osmotic suction (π). Matric suction is usually assumed to be the main component of the total suction in non-plastic soils with a pure pore fluid, while osmotic suction is appreciable in high plastic clays or in cases where the pore fluid contains dissolved salts. According to Carrera *et al.* (2011), Stava silt has been defined as an inorganic silt of low plasticity and compressibility, indicating that osmotic suction represents a small amount of the total suction, so that $\psi \approx s$. Total suctions imposed on tailing specimens were 4.0 MPa, 11.4 MPa, 57 MPa and 70 MPa by K_2SO_4 , KNO_3 , NaNO_2 and $\text{Ca}(\text{NO}_3)_2 \cdot 4\text{H}_2\text{O}$ saturated solutions.

Finally, a chilled mirror psychrometer WP4 was used to measure the total suction along the main drying branch of soil specimens 20 mm initial diameter, 10 mm height. The dew point technique (range: 0-300 MPa; accuracy: ± 0.05 MPa from 0 to 5 MPa, 1% from 5 to 300 MPa) was applied, together with the vapour equilibrium technique, to obtain the water content-suction relationship for high suction values. Immediately after the preparation, samples were exposed at regular intervals to the laboratory atmosphere for a couple of hours. At each step, their total suction was measured with WP4 (equilibrium time: 15-30 minutes) together with the gravimetric water content until reaching equilibrium when no variation in water content and total suction was recorded. The measured total suction ranged from 1 MPa to 150 MPa. The measurement of the total suction by using the dew point technique consists of equilibrating the vapour phase of the water in the air space

above the sample in a closed chamber with the liquid phase of the water within the unsaturated soil specimen (Fig. 8(b)). A cooling system is used to cool a mirror until dew forms. An optical sensor is used to detect the dew formed on the mirror, while a thermocouple attached to the mirror measures the dew point temperature ($\pm 0.2^\circ\text{C}$). In the meantime, the temperature of the unsaturated sample is measured with an infrared thermometer. A fan is also used to circulate the air in the sensing chamber and speed up vapour equilibrium. Both the soil sample temperature and the dew point are employed to obtain the relative humidity above the soil sample and so its total suction according to the psychrometric law.

4. Required variables

The main variables required for the estimation of the water retention curve are summarized in the following.

4.1 Evaluation of the water retention curves

The experimental data were fitted using the water retention model proposed by van Genuchten (1980):

$$Sr = \frac{1}{(1 + (\alpha s)^n)^m} \quad (1)$$

where α is associated to the air entry value AEV of the soil (additional air pressure, with respect to the water pressure, required for air to fill the biggest soil pores during the drying process), while dimensionless, dependent parameters n and $m = 1 - (1/n)$ determine the shape of the curve.

To account for variation of the void ratio on the water retention behaviour, the model proposed by Gallipoli *et al.* (2003) was applied, where dimensionless parameters n , m , ψ and Φ (kPa^{-1}) are soil constants, while ν is the specific volume ($\nu = 1 + e$):

$$Sr = \frac{1}{(1 + [\Phi(\nu - 1)\psi s]^n)^m} \quad (2)$$

Gallipoli parameters ψ and Φ are calibrated from the power law $\alpha = \Phi(\nu - 1)^\psi$ by fitting the points in ($AEV - e$) plane. Those points refer from at least two samples having the same grain size distribution but different void ratios, with the air entry value ($AEV = 1/\alpha$) given by previous best fitting of van Genuchten model. Then, the n parameter is calibrated, so $m = 1 - (1/n)$ is obtained. The detailed procedure is given in Bella (2017).

Defining the residual degree of saturation Sr^{res} as the state in which the water phase within the soil pores is discontinuous and water can be moved through the soil only as water vapour ($Sr^{res} = 0.05$), the effective degree of saturation Sr_{eff} was obtained:

$$Sr_{eff} = \frac{Sr - Sr^{res}}{1 - Sr^{res}} \quad (3)$$

where Sr^{res} is the irreducible (residual) degree of saturation, assumed to be the one determined at the highest suction imposed with the vapour equilibrium technique.

4.2 Evaluation of the pore size density

In order to give a microstructural interpretation of each

water retention curves of the Stava tailings, the water retention was assumed to be due to the capillary mechanism. The pore size density PSD of the soil samples was evaluated by defining a proper range of suction levels s , so its corresponding pore radius r was computed by inversion of Washburn-Laplace equation (Eqs. 4a-4b). Pores with different sizes were assumed to be cylindrical, contact angle α between water and pore's wall equal to 0° and water tension T_s equal to 72 mN/m at temperature of 20°C :

$$r = \frac{2 \cdot T_s \cdot \cos(\alpha)}{s} \quad (4a)$$

$$PSD = \frac{\Delta \left[\frac{e(1 - Sr_{eff})}{Gs} \right]}{\Delta \log(r)} \quad (4b)$$

where Sr_{eff} is the effective degree of saturation evaluated at each suction level by using the van Genuchten model (Eq. (1)) and G_s is the specific weight (Table 1).

5. Experimental results and interpretation

In Section 5.1 and 5.2 the influence of the initial void ratio, preparation technique and fine content on the hydraulic behaviour of samples was investigated by means of water retention tests. Then, the effect of initial density on the PSD of Stava silt samples was analyzed in Section 5.3. It is worth noting that the pore size was not given by mercury intrusion porosimetry tests, but it has been obtained from the theoretical water retention curves.

5.1 Evidences of the influence of the initial density on the water retention behaviour

Fig. 9 shows the experimental results (SILT-0.70) obtained from the three adopted methods: axis translation, dew-point and vapour equilibrium technique. The black triangles are the experimental points obtained from the axis translation technique; the unfilled black squares show the results obtained from the dew-point method, and the unfilled circles show the results from the vapour equilibrium technique. The black diamond marked as “ s_i ?” represents the assumed initial state of the specimen in terms of the degree of saturation and suction value. Indeed, the initial degree of saturation has been imposed (70%) while the initial suction was unknown. Due to the drying response of the sample at the imposed suction 50 kPa at the first step of the water retention test, the initial suction of the sample was less than that suction value. Furthermore, main drying and wetting curves define a domain, so the initial suction ranges between 4 kPa and 30 kPa . Additionally, as shown in the same Fig. 9, suction levels obtained by the vapour equilibrium technique were partially superimposed on those obtained by the dew point technique (redundancy).

Experimental points were fitted using the simplified van Genuchten model to obtain the main drying (solid line) and main wetting branch (dotted line). The drying curve was fitted using experimental points obtained during the drying

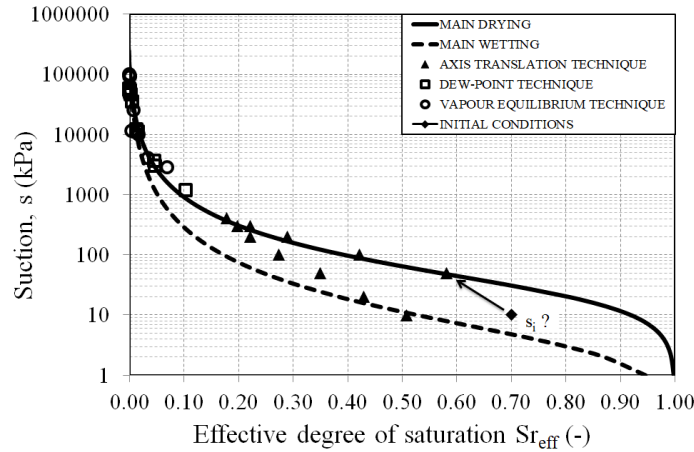


Fig. 9 Sample SILT-0.70: experimental points and fitting curve for the three applied methods

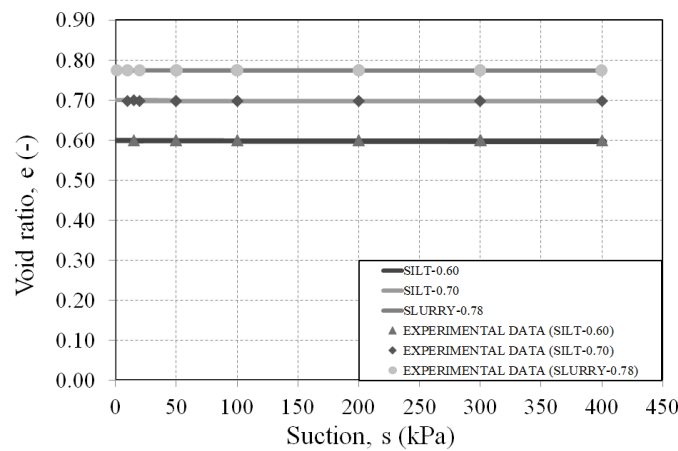


Fig. 10 Void ratio during the water retention tests

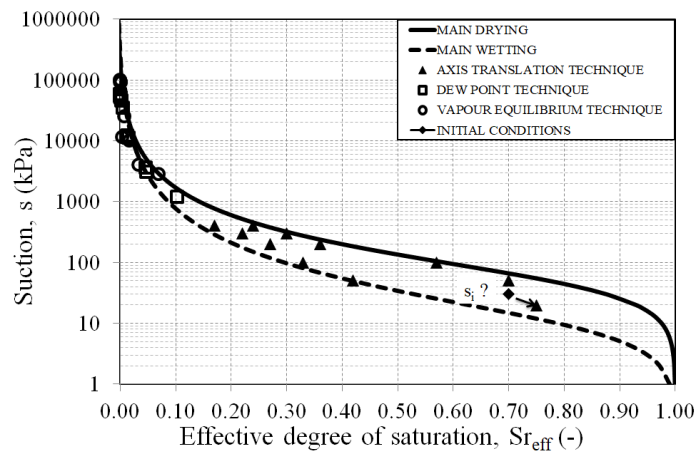


Fig. 11 Sample SILT-0.60: experimental points, fitting curve for the three applied methods

process (axis translation technique, WP4C and VET). It is important to note that, since the specimen in the suction controlled oedometer was dried only up to a maximum suction $s = 400$ kPa, and then wetted, the wetting points in the range $50 \text{ kPa} < s < 300 \text{ kPa}$ do not belong to the main wetting but to a scanning curve. For this reason, the main wetting branch was fitted by assuming just the last two points ($s \leq 50$ kPa) belong to the main wetting curve and by

using points at suction values up to 11.4 MPa (VET/WP4C).

During the water retention tests, void ratio was shown to be constant at different suction steps for the slurry sample (SLURRY-0.78) and for the statically compacted samples (SILT-0.70 and SILT-0.60) as shown in Fig. 10.

Experimental results obtained for sample SILT-0.60 from the three performed methods are shown in Fig. 11.

Table 4 List of the van Genuchten parameters α , n , m and air entry values

Sample	Main drying branch			Main drying branch			AEV (kPa)
	α (kPa ⁻¹)	n (-)	m (-)	α (kPa ⁻¹)	n (-)	m (-)	
SLURRY-0.78	0.030	1.630	0.390	0.280	1.480	0.320	33.3
SILT-0.70	0.042	1.620	0.380	0.320	1.500	0.330	23.8
SILT-0.60	0.019	1.650	0.390	0.100	1.520	0.340	52.6
SILT-0.50	0.009	1.670	0.400	0.065	1.520	0.340	111.1
7030-0.70	0.120	1.550	0.350	0.600	1.700	0.410	8.3
3070-0.60	0.021	1.680	0.400	0.150	1.540	0.350	47.2

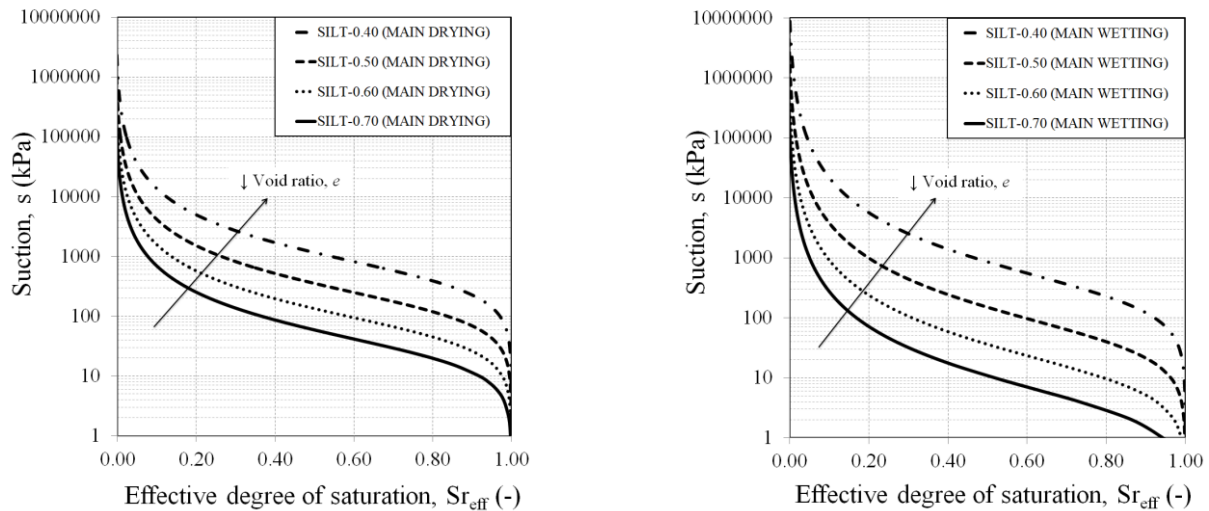


Fig. 12 Influence of void ratio on the water retention behaviour

Again, the black triangles are the results obtained from the axis translation technique; the unfilled squares are the experimental points obtained from the dew-point technique and the unfilled circles are the results obtained from the vapour equilibrium technique. The experimental points were then fitted by the simplified van Genuchten model to obtain the main drying and main wetting branches.

The Van Genuchten fitting parameters for the silt samples and mixtures, both for the main drying and main wetting branch together with the air entry values, are given in Table 4.

The influence of void the ratio on the water retention curve of silty samples with the same grain size distribution, but different initial density, was studied using the Gallipoli model (Fig. 12). The calibration of the Gallipoli parameters, based on the experimental results of SILT-0.70, SILT-0.60, allowed the water retention behavior for a wide range of void ratios, i.e. SILT-0.50 and SILT-0.40 to be obtained. It can be observed that both the main drying and wetting branches are strongly influenced by initial density of the samples. Different void ratios also imply a different pore size distribution, and this affects the hydraulic behaviour in terms of the water retention curve. A decrease in the void ratio shifts the water retention curve to a higher suction because as the size of the pores decreases, a higher suction is required to empty the pores. For this reason, the water retention curve of SILT-0.40, SILT-0.50 and SILT-0.60 rest above the curve of SILT-0.70. The α parameter of Gallipoli

model is related to the inverse of the air entry value, and this was confirmed by the specimen with the lower void ratio ($e_0 = 0.40$) being associated with the smallest value of α . This means that the soil is expected to remain saturated even for a relatively high suction which, although still being a modest value, is still significantly higher than found for the same material with a lower initial density.

A summary of technical literature data depicts the main drying branches of the water retention curves for different types of soils (both tailings and more standard materials) under different compaction states was compiled and is shown in Fig. 13 which highlights the similarities and differences with the results from the current research.

Fig. 13(a) shows the best fitting water retention curves obtained from nickel tailing samples, from the Pedro Sotto Alba tailings impoundment (Cuba) with different compaction states ($e_i = 1.00$, $e_i = 0.75$, $e_i = 0.50$). Fig. 13b shows the WRC for different initial void ratios ($e_i = 1.18$, $e_i = 1.13$, $e_i = 1.08$) on Pearly clay specimens for a suction range between 10 kPa and 200 kPa. Figure 10c shows the WRC obtained from a compacted clayey silt at three different initial void ratios ($e_i = 1.00$, $e_i = 0.75$, $e_i = 0.50$), while Fig. 13(d) gives the main drying water retention curves at different compaction states ($e_i = 1.46$, $e_i = 0.93$, $e_i = 0.64$, $e_i = 0.59$) for Boom clay specimens. These data from literature, for both for tailing materials (Fig. 13(a)) and more standard soils (Fig. 13(b)-13(d)) show a good agreement with results of the water retention tests obtained

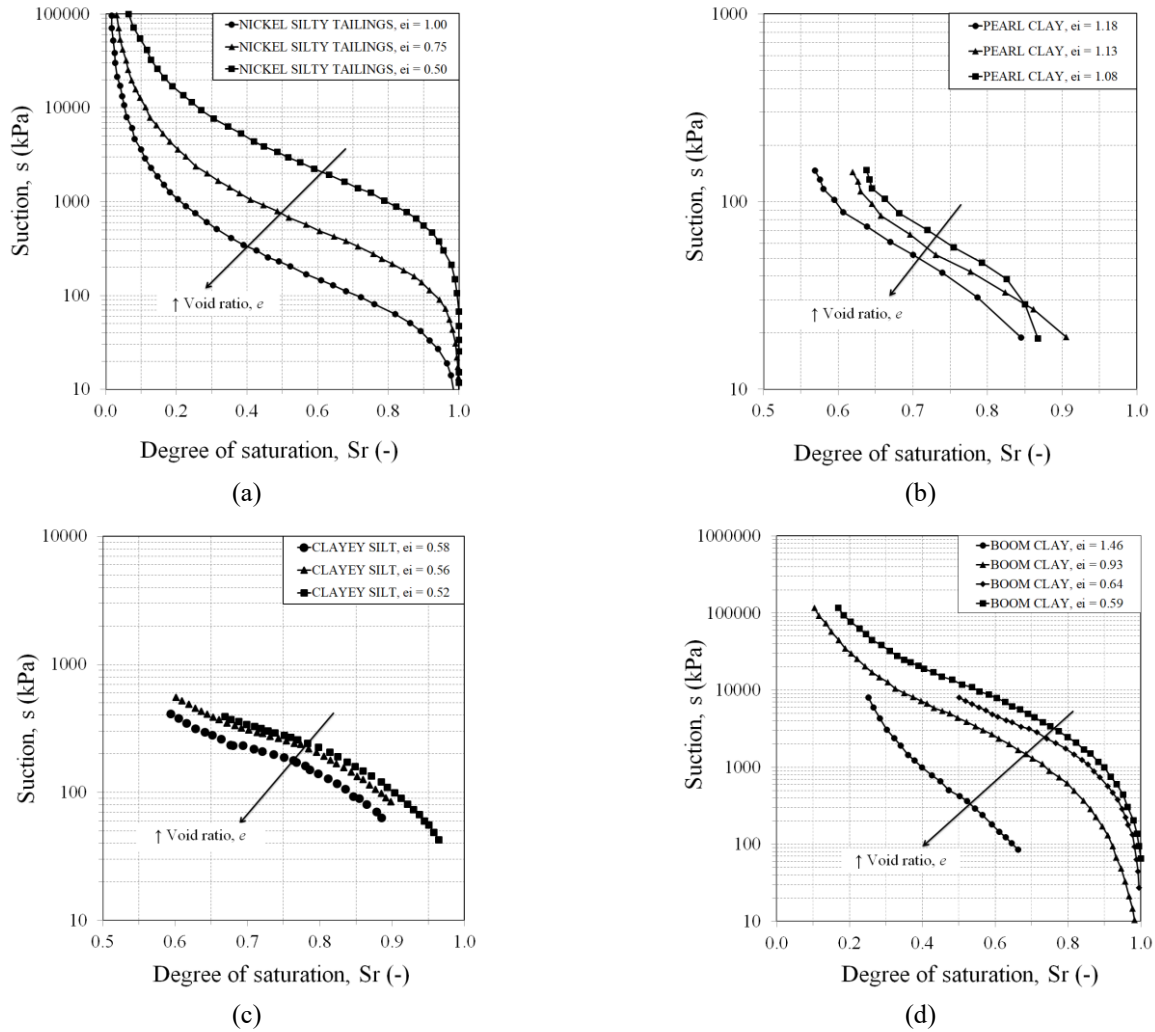


Fig. 13 Water retention curves for different type of soils and initial void ratio e_i : (a) Nickel tailings modified from Zanardin *et al.* (2009), (b) Pearl clay, modified from Sun *et al.* (2007), (c) Clayey silt, modified from Vanapalli *et al.* (1999) and (d) Boom clay, modified from Romero (1999).

in this research on the Stava tailings at different compaction states (Fig. 12). Within the suction range investigated for both these cases, the water retention curves were shifted upward with decreasing the initial void ratio of compacted soil. As shown in this research and the literature data for standard soils (Fig. 13), except for the very loose Boom clay specimen $e_i = 1.46$, variations in void ratio variations do not affect the shape of the WRC significantly. This is confirmed by n , m parameters for SILT-0.70, SILT-0.60 and SILT-0.50, for the main drying and wetting branches (Table 4).

5.2 Evidences of the influence of the preparation techniques and fine content on the water retention behaviour

Table 5 provides the Gallipoli fitting parameters for silty samples, both for the main drying and wetting branches.

A preliminary evaluation of the influence of the preparation technique was investigated by best fitting the experimental points of SLURRY-0.78. If the experimental points of SLURRY-0.78 were fitted to both the van

Table 5 List of the Gallipoli retention parameters n , m , Φ and ψ for silty samples

Main drying branch				Main wetting branch			
n (-)	m (-)	Φ (-)	ψ (-)	n (-)	m (-)	Φ (-)	ψ (-)
1.670	0.400	0.281	5.327	1.500	0.330	5.405	7.810

Genuchten model and Gallipoli model, and a relevant difference was observed. The van Genuchten model (solid and dotted grey lines) predicts the water retention behaviour of SLURRY-0.78 well. Otherwise, if the same experimental points are fitted using the Gallipoli model (solid and dotted black lines) based on the same calibrated parameters used for statically compacted SILT-0.70, SILT-0.60 (Fig. 14(a)), a significant difference is appreciated. This means that, also for tailings, the water retention behaviour is strongly affected by the soil structure that, in turns, is influenced by the preparation technique. As shown in Fig. 14a, the slurry sample shows a greater water retention capability than the static compacted sample, and this probably depends on the different pore size distributions of the samples obtained

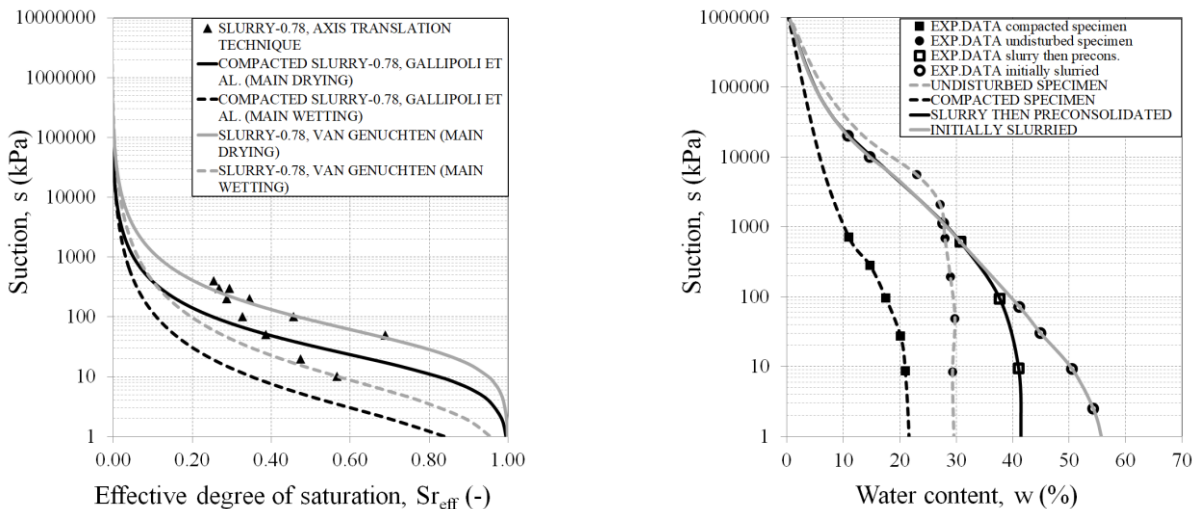


Fig. 14 Influence of the preparation technique on the water retention behaviour: (a) Stava tailings tested in this research and (b) standard soils (modified from Fredlund and Pham 2006)

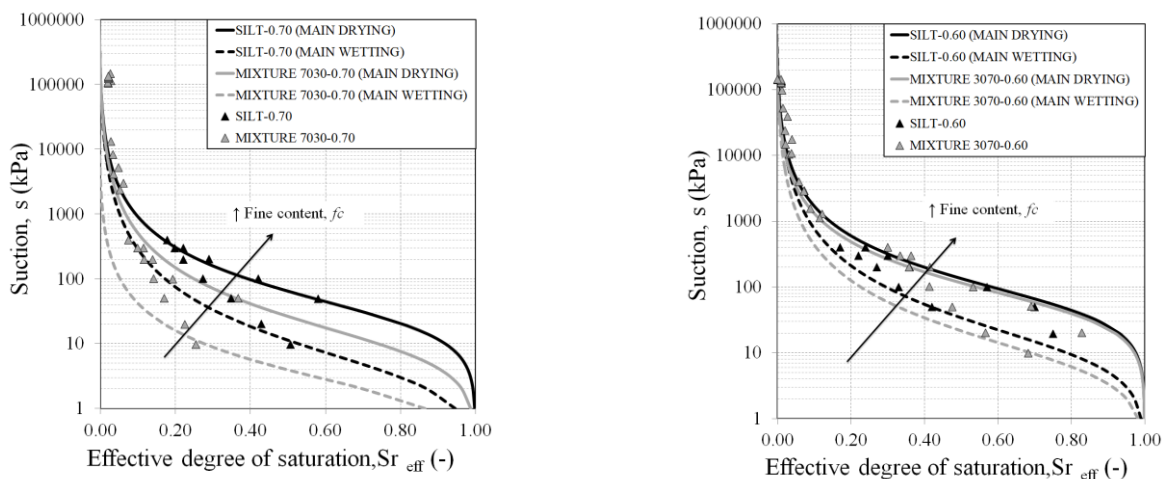


Fig. 15 Influence of the fine content on the water retention behaviour

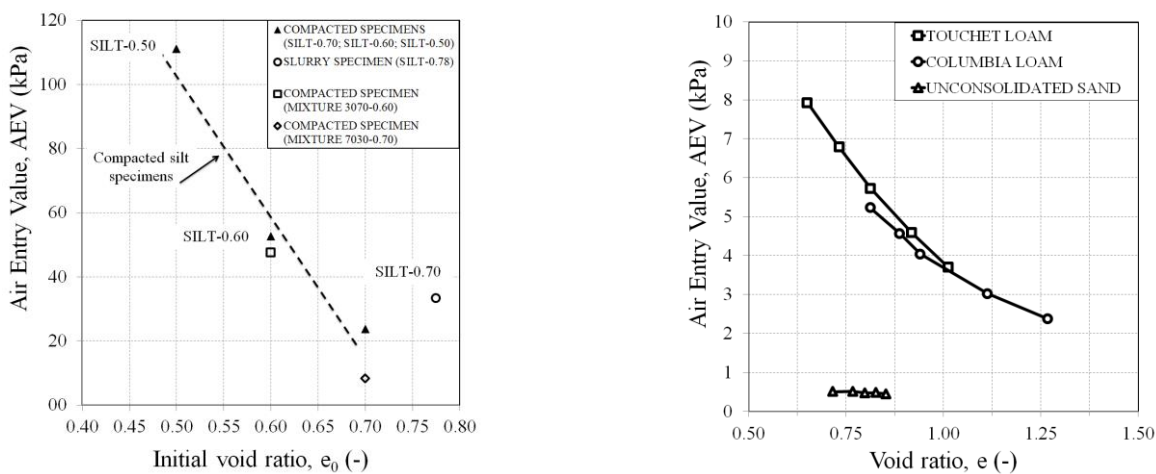


Fig. 16 Influence of the void ratio and preparation method with air entry value: (a) Stava tailings tested in the current research and (b) standard soils (modified from Huang *et al.* 1998)

from the two preparation methods. The outcomes obtained in this research on the Stava tailings are found to be in good

agreement with the literature results of water retention tests carried out on more standard soils. According to Fredlund

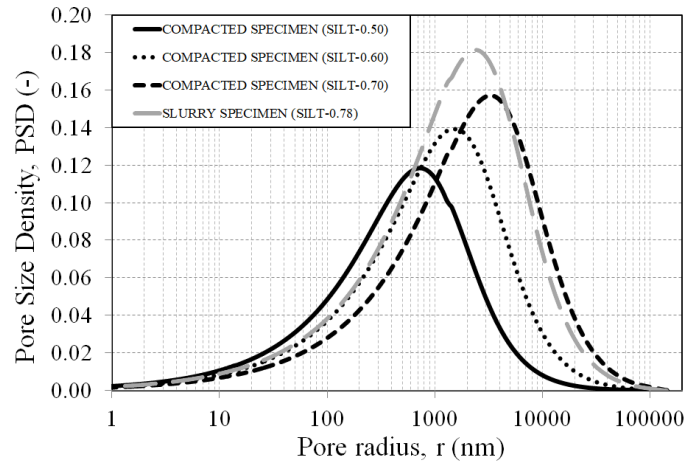


Fig. 17 Influence of the void ratio and preparation technique on the pore size density

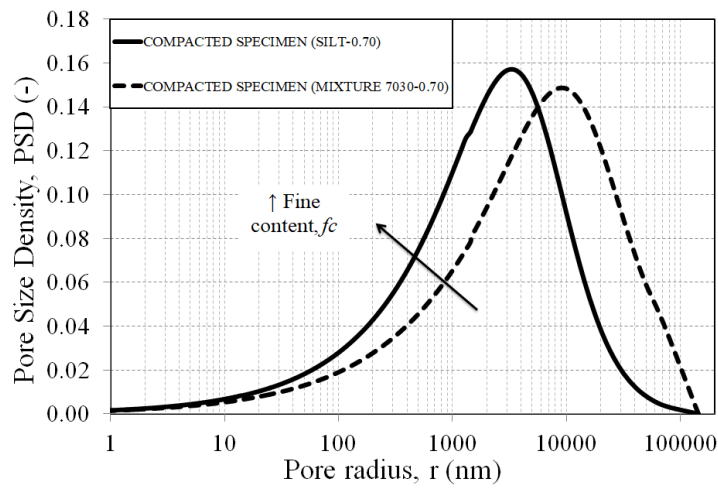


Fig. 18 Influence of the fine content on the pore size density ($e_0 = 0.70$)

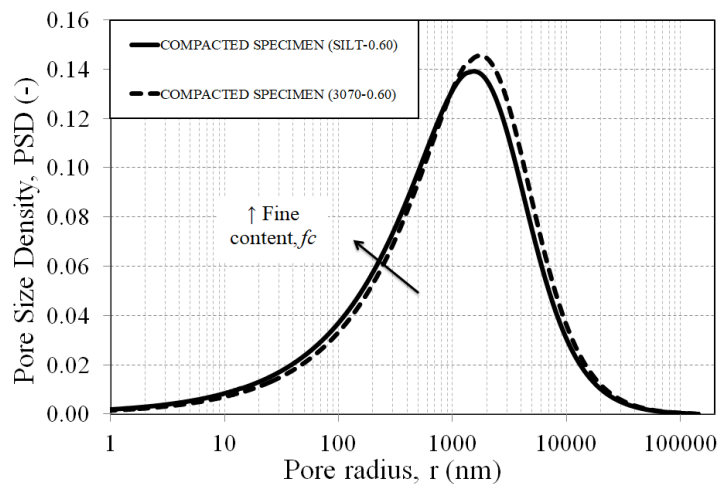


Fig. 19 Influence of the fine content on the pore size density ($e_0 = 0.60$)

and Pham (2006), and Pham and Fredlund (2008), the soil-water characteristic curves differ, depending on the applied historical stresses and hence on the initial state of the specimen (Fig. 14(b)). It is worth noting that, due to the coupling between hydraulic and mechanical behaviour in

unsaturated conditions, the mechanical response in terms of liquefaction strength was also proved to be influenced by the preparation technique, for both tailings (i.e., Chu *et al.* 2003, Bella 2017), and standard soils (i.e., Vaid and Sivathayalan 2000).

The influence of the fine content on the water retention behaviour was also studied. Soil-water characteristic curves of tailing samples prepared with the same initial density, but with different fine content were compared as shown in Fig. 15a (SILT-0.70 with 7030-0.70) and Fig. 15b (SILT-0.60 with 3070-0.60). In both the pure silt (SILT-0.70 and SILT-0.60) and mixtures samples (3070-60 and 7030-0.70), the main drying and wetting branches of the WRC were affected by changes in grain size distribution. At an increase of fine content, correspond a movement of the water retention curve to high suction values. Indeed, when increasing the fine content, the pores between the sandy particles get filled with the small silty particles resulting an overall lower permeability, and so a higher retention behaviour. A comparison of the air entry values of the two samples having the same initial void ratio ($e_0 = 0.70$) but high difference in fine content show that the AEV of SILT-0.70 (23.8 kPa) is higher than that of sample 7030-0.70 (8.3 kPa). This means that, despite the same initial compaction state, the tailing mixture can be desaturated by applying a smaller suction than that required for the pure silt as, the latter one is expected to have small pores. Similar considerations were done by comparing the water retention behaviour of sample SILT-0.60 with mixture 3070-0.60. Due to the small difference in fine content, both the main drying and wetting branches were only slightly affected by changes in the grain size distribution. The values of the α parameter are 0.019 kPa^{-1} for the pure silt and 0.021 kPa^{-1} for the silt-sand mixture. This corresponds to the AEV of 52.6 kPa and 47.2 kPa respectively, indicating that the pure silt fraction can be desaturated by imposing a higher suction than the sand-silt mixture. Indeed, at the same void ratio the sand-silt mixture is expected to have fewer but larger pores than the silt material.

The influence of the initial density on the water retention behaviour was also observed by the decrease in the air entry value with the increase in void ratio for the statically compacted silt samples (Fig. 16(a), dotted line). Indeed, a lower pressure (suction) is required to fill the bigger empty pores of the looser samples with air. The importance of the pore size distribution on the water retention behaviour was also investigated by comparing the air entry value of the silt sample SILT-0.70 with the air entry value of the mixture 7030-70 both with an initial void ratio $e_0 = 0.70$ (Fig. 16, black triangle at $e_0 = 0.70$ and unfilled diamond). Again, a lower pressure is required to fill the bigger empty pores of the mixtures with air. Similar considerations were done by analyzing the air entry value of the silt sample SILT-0.60 with the air entry value of the mixture 3070-60, both with an initial void ratio $e_0 = 0.60$ (Fig. 16(a): black triangle and unfilled square). Moreover, the influence of the preparation technique on the hydraulic behaviour was observed by comparing the dotted line showing the trend of the air entry value of statically compacted samples (Fig. 16a, dotted line) with the air entry value of SLURRY-0.78 (Fig. 16a, empty circle). Due to the different preparation technique, the soil structure was different and the air entry value of SLURRY-0.78 was not aligned with those of the statically compacted samples.

The dependency of the air entry value on the porosity of

“standard soils” has been quantified in a number of relatively recent publications (Huang *et al.* 1998; Vanapalli *et al.* 1999; Ng and Pang, 2000; Cabarkapa and Cuccovillo, 2006) showing good agreement with the experimental results obtained in this research on the Stava tailings. Some literature data depicting the evolution of the air entry value with void ratio for different type of soils, loam and sand under different compaction states was shown in Fig. 16b. As for Stava tailings, it was noticed that, for a given material, the AEV increases with decreasing voids, and at a given void ratio the air entry value was more than ten times higher for the loams than that for the sands.

5.3 Evidences of the influence of the initial density, preparation techniques and fine content on the pore size density

A preliminary microstructural interpretation of the different water retention curves of the Stava tailings at different initial densities and grading was performed by assuming that the water retention was due to the capillary mechanism described by the Washburn-Laplace equation. The effect of void ratio on the pore size density was investigated by comparing the pore size distributions of silt samples with different initial density, i.e. SILT-0.70, SILT-0.60 and SILT-0.50 (Fig. 17). The pore size density peak of SILT-0.70 occurs at a larger pore radius than those of SILT-0.60 and SILT-0.50. This is consistent with their estimated air entry values given in Fig 13. Moreover, the pore size density curve of SILT-0.70 was wider than those of samples SILT-0.60 and SILT-0.50. This means that looser sample SILT-0.70 has a larger range of pores size than SILT-0.60 and SILT-0.50, so that SILT-0.70 sample has a lower water retention capability than the other two samples. These considerations were not identified for SLURRY-0.78, suggesting the influence that the preparation technique has on the water retention behaviour.

The effect of grain size distribution on the pore size density was observed from the comparison of the tailing samples having the same initial density but different sand-silt percentages, i.e. SILT-0.70 and 7030-0.70 (Fig. 18). Due to the higher fraction of sand in sample 7030-0.70 than in SILT-0.70, it is expected that the mixture was more permeable than the latter. The air entry value of 7030-0.70 was lower than that of SILT-0.70 (Tab. 4) and this implies that the lower the air entry value is, the higher the permeability is. As expected, the highly permeable sample 7030-0.70 having many pores, also of large size, required a lower pressure to fill them. As shown in Fig. 18 the pore radius peak of 7030-0.70 occurred at a higher pore radius than that of SILT-0.70 which is consistent with their respective AEVs.

Similar considerations were accomplished by comparing another pair of samples having the same initial density but different grain size distribution, i.e. SILT-0.60 with 3070-0.70 (Fig. 19). Again, an increase in the fine content shifted the pore size density curve toward the smaller pore radius.

6. Conclusions

Tailing dams, because of their large spatial extension,

long operational-life, raising methods, depositional techniques, that have resulted in a high number of unacceptable failure (both socially and environmentally detrimental), need detailed investigations during the design phases and regular monitoring during the operational phases. Due to the hydro-mechanical coupling in unsaturated soils, the hydraulic response of tailings affects the stability of tailing dams in terms of resistance properties. Indeed, shear strength changes with suction, that in turn is related to the degree of saturation by means of the WRC. So, an accurate prediction of the hydraulic behaviour within the unsaturated layers above the phreatic surface has a significant effect on the mechanical response, particularly regarding the consequences of the stability of tailing dams. This research has provided, in unsaturated conditions, a preliminary characterization of tailing materials collected from the Stava basins, outlining the effects of void ratio, particle sorting and preparation technique on their hydraulic behaviour. Several experimental techniques were adopted to characterise the dependency of the water retention behaviour within a wide suction level as follows:

- The water retention behaviour of Stava silty samples with the same grain size distribution but different initial density was studied by comparing their WRC. This condition has a practical relevance in modelling the hydro-mechanic behaviour of tailings because it could represent different depths of a unique vertical cross section at the same distance from the embankment. The increase in void ratio was proved to shift the water retention curve to a lower suction range because the size of the pores increases. A lower suction is therefore required to empty the pores, leading to a lower water retention capability in loose unsaturated tailing than denser ones.

- The hydraulic response of unsaturated tailing mixtures with the same initial void ratio but different fine content was investigated by analysing their water retention curves. This condition has a practical relevance since it could represent the same depth for several vertical cross sections located at the different distance from the embankment. Also for Stava tailings, an increase of the fine content was proved to move the water retention to higher suction values as the big pores between sandy particles get filled with small silty particles, leading to a higher water retention capability of pure silt samples than that of silt-sand mixtures.

- The influence of the preparation technique was preliminary studied by comparing the WRC of a slurry sample with those that obtained from a statically compacted specimen. The slurry sample shows a greater water retention capability than that of the same sample created from static compaction method due to the different pore size distribution of the two preparation techniques.

- The use of several types of non-standard, sophisticated equipment, the time-consuming experimental methodologies, as well as the use of the axis translation, the vapour equilibrium method and the chilled-mirror psychrometer, were shown to be the best way to investigate the hydraulic behaviour of unsaturated tailings in order to perform reliable stability analysis.

- The experimental results on Stava tailings provided by

water retention tests were successfully compared with the results described in literature on standard soils.

- A microstructural interpretation of the water retention capability of the Stava tailings was shown in terms of pore size distribution by assuming that the water retention was due to the capillary mechanism described by the Washburn-Laplace equation.

Following the results obtained in this study, further research could cover a larger domain of void ratios as well as other mixtures made up of sandy and silty tailings to different percentages to simulate the heterogeneity of in situ tailings. Finally, it was observed that the real environment is more complex than the conditions reproduced during the experimentation. Experimentation was adopted to simplify the experimental program, as at the site the tailings are mixed with water which contains dissolved salts, heavy metals, contaminants, and residual chemicals from the mineralogical processes. To simulate the real environment more accurately, more retention tests could be carried out by using processing water or by considering the aging effects related to the particle rearrangements that result in the macro-interlocking or the cementation of the particles.

Acknowledgments

The Author wishes to thank Prof. G. Musso, M. Barbero and F. Barpi (Politecnico di Torino) for their valuable inputs, suggestions and support while analyzing the experimental data. The Author also wishes to acknowledge Dr. A. Azizi, Dr. O. Pallara and Mr. G. Bianchi for their help during the laboratory tests presented in this work.

References

- Alonso, E.E., Gens, A. and Josa, A. (1990), "A constitutive model for partially saturated soils", *Géotechnique*, **40**(3), 405-430. <https://doi.org/10.1680/geot.1990.40.3.405>.
- Alonso, E.E. and Gens, A. (2006), "Azna collar dam failure. Part I: Field observations and material properties", *Geotechnique*, **56**(3), 165-183. <https://doi.org/10.1680/geot.2006.56.3.165>.
- Alonso, E.E., Pereira, J.M., Vaunat, J. and Olivella, S. (2010), "A microstructurally based effective stress for unsaturated soils", *Geotechnique*, **60**(12), 913-925. <http://doi.org/10.1680/geot.8.P.002>.
- Arab, A., Belkhatir M. and Sadek, M. (2015), "Saturation effect on behaviour of sandy soil under monotonic and cyclic loading: A laboratory investigation", *Geotech. Geol. Eng.*, **34**(1), 347-358. <https://doi.org/10.1007/s10706-015-9949-6>.
- Bella, G. (2017), "Hydro-mechanical behaviour of tailings in unsaturated conditions", Ph.D. Dissertation, Politecnico di Torino, Torino, Italy.
- Bhanbhro, R. (2014), "Mechanical properties of tailings - basic description of a tailings material from Sweden", Ph.D. Dissertation, Luleå University of Technology, Luleå, Sweden.
- Bulut, R., Hineidi, S.M. and Bailey, B. (2002), "Suction measurements - filter paper and chilled mirror psychrometer", *Proceedings of the Texas Section American Society of Civil Engineers*, Waco, Texas, U.S.A., October.
- Cabarkapa, Z. and Cuccovillo, T. (2006), "Automated triaxial apparatus for testing unsaturated soils", *Geotechnical Testing Journal*, **29**(1), 21-9. <https://doi.org/10.1520/GTJ12310>.

- Carrera, A., Coop, M. and Lancellotta, R. (2011), "Influence of grading on the mechanical behaviour of Stava tailings", *Geotechnique*, **61**(11), 935-946. <https://doi.org/10.1680/geot.9.P.009>.
- Chandler, R.J. and Tosatti, G. (1995), "The Stava tailings dams failure, Italy, July 1985", *Proc. Inst. Civ. Eng. Geotech. Eng.*, **113**(2), 67-79. <https://doi.org/10.1680/igeng.1995.27586>.
- Chu J., Leong, W.K. and Loke, W.L. (2003), "Discussion of "defining an appropriate steady state line for Marriespruit gold tailings", *Can. Geotech. J.*, **40**(2), 484-486. <https://doi.org/10.1139/t02-118>.
- Deng, D., Wen, S., Lu, K. and Li, L. (2020), "Calculation model for the shear strength of unsaturated soil under nonlinear strength theory", *Geomech. Eng.*, **21**(3), 247-258. <https://doi.org/10.12989/gae.2020.21.3.247>.
- Esposito, T., Assis, A. and Giovannini, M. (2010), "Influence of the variability of geotechnical parameters on the liquefaction potential of tailing dams", *Int. J. Surface Min. Reclam. Environ.*, **16**(4), 304-316. <https://doi.org/10.1076/ijsm.16.4.304.8639>.
- Estabragh, A.R. and Javadi, A.A. (2014), "Roscoe and Hvorslev Surfaces for Unsaturated Silty Soil", *Int. J. Geomech.*, **14**(2), 230-238. [https://doi.org/10.1061/\(ASCE\)GM.1943-5622.0000306](https://doi.org/10.1061/(ASCE)GM.1943-5622.0000306).
- Fredlund, D.G., Morgenstern, N.R., and Widger, R.A. (1978), "The shear strength of unsaturated soils", *Can. Geotech. J.*, **15**(3), 313-321. <https://doi.org/10.1139/t78-029>.
- Fredlund, D.G., Xing, A., Fredlund, M.D. and Barbour, S.L. (1996), "The relationship of the unsaturated soil shear strength to the soil-water characteristic curve", *Can. Geotech. J.*, **33**(3), 440-448. <https://doi.org/10.1139/t96-065>.
- Fredlund, D.G., and Pham, Q.H. (2006), "A volume-mass constitutive model for unsaturated soils in terms of two independent stress state variables", *Proceedings of the 4th International Conference on Unsaturated Soil*. Carefree, Arizona, U.S.A., April.
- Gallipoli D., Wheeler, S.J. and Karstunen M. (2003), "Modelling the variation of degree of saturation in a deformable unsaturated soil", *Geotechnique*, **53**(1), 105-112. <https://doi.org/10.1680/geot.2003.53.1.105>.
- Gan, J.K.M., Fredlund, D.G., and Rahardjo, H. (1988), "Determination of the shear strength parameters of an unsaturated soil using the direct shear test", *Can. Geotech. J.*, **25**(3), 500-510. <https://doi.org/10.1139/t88-055>.
- Horn-Da, L., Chien-Chih, W. and Xu-Hui, W. (2018), "A simplified method to estimate the total cohesion of unsaturated soil using an UC test", *Geomech. Eng.*, **16**(6), 599-608. <https://doi.org/10.12989/gae.2018.16.6.599>.
- Huang, S.Y., Barbour, S.L., Fredlund, D.G. (1998), "Development and verification of a coefficient of permeability function for a deformable unsaturated soil", *Can. Geotech. J.*, **35**(3), 411-425. <https://doi.org/10.1139/t98-010>.
- Khalili, N. and Khabbaz, M.H. (1998), "A unique relationship for χ for the determination of the shear strength of unsaturated soils", *Géotechnique*, **48**(5), 681-687. <https://doi.org/10.1680/geot.1998.48.5.681>.
- Kim, Y., and Jeong, S. (2017), "Modeling of shallow landslides in an unsaturated soil slope using a coupled model", *Geomech. Eng.*, **13**(2), 353-370. <https://doi.org/10.12989/gae.2017.13.2.353>.
- Lu, N. and Likos, W.J. (2006), "Suction stress characteristic curve for unsaturated soil", *J. Geotech. Geoenviron. Eng.*, **132**(2), 131-142. [https://doi.org/10.1061/\(ASCE\)1090-0241\(2006\)132:2\(131\)](https://doi.org/10.1061/(ASCE)1090-0241(2006)132:2(131)).
- Lucchi, G. (2021), "Tailing Dams: lezioni dal passato e dal presente. Stava: Cause e responsabilità[Tailing Dams: lessons learnt from the past and present: Causes and responsibilities"]", *Online Conference*, GEAM.
- Luino, F. and De Graff, J.V. (2012), "The Stava mudflow of 19 July 1985 (Northern Italy): A disaster that effective regulation might have prevented", *Nat. Hazards Earth Syst. Sci.*, **12**, 1029-1044. <https://doi.org/10.5194/nhess-12-1029-2012>.
- Ng, C.W.W. and Pang, Y.W. (2000), "Influence of stress state on soil-water characteristics and slope stability", *J. Geotech. Geoenviron. Eng.*, **126**(2), 157-66. [https://doi.org/10.1061/\(ASCE\)1090-0241\(2000\)126:2\(157\)](https://doi.org/10.1061/(ASCE)1090-0241(2000)126:2(157)).
- Nicotera, M.V., Papa, R. and Urciuoli, G., (2015), "The hydro-mechanical behaviour of unsaturated pyroclastic soils: An experimental investigation", *Eng. Geol.*, **195**, 70-84. <https://doi.org/10.1016/j.enggeo.2015.05.023>.
- Öberg A.L. and Sallfors, G. (1997), "Determination of shear strength parameters of unsaturated silts and sands based on the water retention curve", *Geotech. Test. J.*, **20**(1), 40-48. <https://doi.org/10.1520/GTJ11419J>.
- Pham H.Q. and Fredlund, D.G. (2008), "Equations for the entire soil-water characteristic curve of a volume change soil", *Can. Geotech. J.*, **45**(4), 443-453. <https://doi.org/10.1139/T07-117>.
- Rassam, D.W. and Cook, F.J. (2002), "Predicting the shear strength envelope of unsaturated soil", *Geotech. Test. J.*, **25**(2), 215-220. <https://doi.org/10.1520/GTJ11365J>.
- Rassam, D.W. and Williams, D.J. (1999), "A relationship describing the shear strength of unsaturated soils", *Can. Geotech. J.*, **36**(2), 363-368. <https://doi.org/10.1139/t98-102>.
- Rico, M., Benito, G., Salgueiro, A.R., Diez-Herrero, A. and Pereira, H.G. (2008), "Reported tailings dam failures - A review of the European incidents in the worldwide context", *J. Hazard. Mater.*, **152**(2), 846-852. <https://doi.org/10.1016/j.jhazmat.2007.07.050>.
- Robertson, P.K., de Melo, L., Williams D.J. and Wilson, G.W. (2019), *Report of the Expert Panel on the Technical Causes of the Failure of Feijão Dam I*.
- Romero, E. (1999), "Thermo hydro-mechanical behaviour of unsaturated Boom Clay: An experimental study", Ph.D. Dissertation, Universidad Politecnica de Catalunya, Barcelona, Spain.
- Santamarina, J.C., Torres-Cruz, L.A. and Bachus, R.C. (2019), "Why coal ash and tailings dam disasters occur", *Science*, **364**(6440), 526-528. <https://doi.org/10.1126/science.aax1927>.
- Sheng, D., Fredlund, D.G., and Gens, A. (2008), "A new modelling approach for unsaturated soils using independent stress variables", *Can. Geotech. J.*, **45**(4), 511-534. <http://doi.org/10.1139/T07-112>.
- Sun, D.A., Matsuoka, H., Yao, Y.P. and Ichihara, W. (2000), "An elasto-plastic model for unsaturated soil in three-dimensional stresses", *Soils Found.*, **40**(3), 17-28. http://doi.org/10.3208/sandf.40.3_17.
- Sun, D., Sheng, D. and Xu, Y. (2007), "Collapse behaviour of unsaturated compacted soil with different initial densities", *Can. Geotech. J.*, **44**(6), 673-686. <https://doi.org/10.1139/t07-023>.
- Tang, A.M. and Cui, Y.J. (2005), "Controlling suction by the vapour equilibrium technique at different temperatures and its application in determining the water retention properties of MX80 clay", *Can. Geotech. J.*, **42**(1), 287-296. <https://doi.org/10.1139/t04-082>.
- Tarantino, A. and Tombolato, S. (2005), "Coupling of hydraulic and mechanical behaviour in unsaturated compacted clay", *Géotechnique*, **55**(4), 307-317. <https://doi.org/10.1680/geot.2005.55.4.307>.
- Tarantino, A. and Mountassir, G. (2013), "Making unsaturated soil mechanics accessible for engineers: Preliminary hydraulic-mechanical characterisation & stability assessment", *Eng. Geol.*, **165**, 89-104. <https://doi.org/10.1016/j.enggeo.2013.05.025>.
- Tarantino, A. and Di Donna, A. (2019), "Mechanics of unsaturated soils: simple approaches for routine engineering practice", *Rivista Italiana Geotec.*, **53**(4), 5-46.

- <https://doi.org/10.19199/2019.4.0557-1405.005>.
- Tekinsoy, M.A., Kayadelen, C., Keskin, M.S. and Soylemez, M. (2004), "An equation for predicting shear strength envelope with respect to matric suction", *Comput. Geotech.*, **31**(7), 589-593. <https://doi.org/10.1016/j.compgeo.2004.08.001>.
- Toll, D.G. (1990), "A framework for unsaturated soil behaviour", *Géotechnique*, **40**(1), 31-44. <https://doi.org/10.1680/geot.1990.40.1.31>.
- Toll, D.G. and Ong, B.H. (2003), "Critical-state parameters for an unsaturated residual sandy clay", *Geotechnique*, **53**(1), 93-103. <https://doi.org/10.1680/geot.2003.53.1.93>.
- Vaid, Y.P. and Sivathayalan, S. (2000), "Fundamental factors affecting liquefaction susceptibility of sands", *Can. Geotech. J.*, **37**(3), 592-606. <https://doi.org/10.1139/t00-040>.
- Vanapalli, S.K., Fredlund, D.G., Pufahl D.E. and Clifton, A.W. (1996), "Model for the prediction of shear strength with respect to soil suction", *Can. Geotech. J.*, **33**(3), 379-392. <https://doi.org/10.1139/t96-060>.
- Vanapalli, S.K., Fredlund D. and Pufahl, D.E. (1999), "The influence of soil structure and stress history on the soil-water characteristics of a compacted till", *Geotechnique*, **49**(2), 143-59. <https://doi.org/10.1680/geot.1999.49.2.143>.
- van Genuchten, M.T. (1980), "A closed-form equation for predicting the hydraulic conductivity of unsaturated soil", *Soil Sci. Soc. Amer. J.*, **44**, 892-898. <https://doi.org/10.2136/sssaj1980.03615995004400050002x>.
- Xu, Y.F. (2004), "Fractal approach to unsaturated shear strength", *J. Geotech. Geoenviron. Eng.*, **130**(3), 264-273. [http://doi.org/10.1061/\(ASCE\)1090-0241\(2004\)130:3\(264\)](http://doi.org/10.1061/(ASCE)1090-0241(2004)130:3(264)).
- Zanardin, M.T., Oldecop, L.A., Rodriguez, R. and Zabala, F. (2009), "The role of capillary water in the stability of tailing dams", *Eng. Geol.*, **105**(1-2), 108-118. <https://doi.org/10.1016/j.enggeo.2008.12.003>.
- Zuoan, W., Yulong C., Guangzhi, Y., Yonghao, Y. and Weimin, S. (2019), "An alternative upstream method for the Zhelamuqing tailings impoundment construction of a Copper Mine in China", *Geomech. Eng.*, **19**(5), 383-392. <https://doi.org/10.12989/gae.2019.19.5.383>.